Light Metals 2008
Edited by: David H. DeYoung
TMS (The Minerals, Metals & Materials Society), 2008

Inclusion Transport Phenomena in Casting Furnaces

Stephen Instone[1], Andreas Buchholz[1] and Gerd-Ulrich Gruen[1]
[1]Hydro Aluminium Deutschland GmbH, Georg-von-Boeselager-Str. 21, 53117 Bonn, Germany

Keywords: simulation, metal quality, settling, inclusions

Abstract

The presence of non-metallic inclusions in Aluminium is one of the most important factors determining its processibility and the quality of finished products. The concentration of such inclusions in the liquid metal has been observed to vary greatly. To better understand the contribution of furnace processes to melt quality, a mathematical model of casting furnace processes has been developed at RDB, Bonn, Germany. The model is capable of simulating the most important fluid flow and particle (inclusion) transport phenomena occurring in the furnace during both settling and casting operations. Output from the model is compared with results from standard inclusion measurement techniques (LiMCA and PoDFA) for different furnace geometries. The model is a powerful tool to improve understanding of these processes and is helpful in explaining observations in the cast house.

Introduction

Process optimization plays an increasingly important role in maintaining competitiveness within the cast house. Optimization of furnace operations is central to an improved cost position in many cast houses. Critical evaluation of design aspects of the furnaces can also yield valuable information related to their cost effective operation. One aspect that can become neglected due to the continuous focus on cost minimization is the quality of the metal that is produced in a particular furnace.

Furnace operations in combination with appropriate in-line refinement steps (degassing, filtration, etc.) determine the quality of the cast products and to a large extent their suitability for downstream processing and application. A good understanding of the effect of the furnace operations is important to control costs but is equally important to ensure the quality of the products produced is sufficient for the demands of downstream processing and end user applications.

A study of the influence of furnace design and operation has been conducted with the assistance of computer modeling of the important physical processes to develop an understanding of the behaviour of un-dissolved inclusions in the furnace during charge preparation and casting. The discussion here will be limited to initial results of the simulation work describing the behaviour of particles in the melt during tilting of the furnace.

Physical Data

Particles

A general description of the type, physical form, size and amount of non metallic, un-dissolved inclusions present in a melting or holding furnace was based on several measurement campaigns in different furnaces using both LiMCA and PoDFA techniques. Typical inclusions and their physical properties are given in Table 1. The general form of the particle size distribution is shown in Figure 1 for both stirred and quiescent melts. Surprisingly the relative proportion of the various particle sizes appeared to be independent of the amount of movement within the bath: quiescent or turbulent conditions in the melt.

Table 1. Typical inclusions and their physical properties

Type of Inclusion:	Density (kg/m³)	Size (µm)	Appearance/Form
		min-max	
Chloride Inclusions	2000	1-20	Circular
Aluminium Carbide	2360	1-10	Square
Alpha-Al2O3	3970	10-100	Variable
Oxide Films	3700	1-50	Stringers
Magnesium Oxide	3800	1-300	Equiaxed/clusters
Al- Mg Spinel Oxide	3600	1-50	Films
Iron Oxide	5750	10-200	Irregular

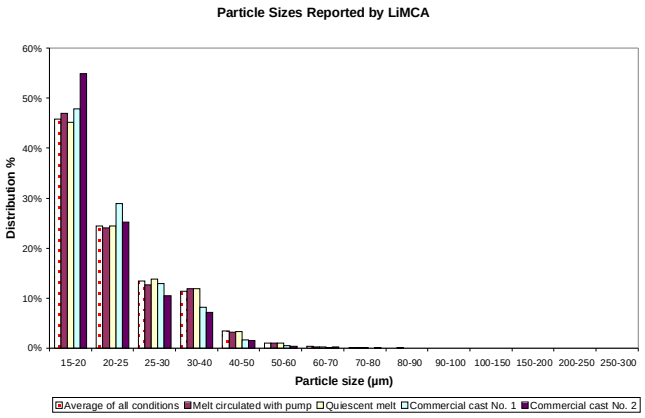

Figure 1. Typical particle size distribution in commercial purity Aluminium melting and holding furnaces.

Furnace Geometry

The furnace geometry used in these simulations is shown in Figure 2. This geometry was chosen as the tilt axis is somewhat unusual in that the furnace tilts around the short axis of the furnace. As a result the floor of the furnace is exposed to the atmosphere due to being lifted above the furnace spout at a relatively low tilt angle. Progressively more of the floor is then exposed as the furnace continues to tilt. An effective simulation should be able to describe the influences of furnace geometry and motion on particle movement within the melt. The capacity of this furnace is approximately 45 metric tons.

Numerical Model

To study particle transport in furnaces a simplified numerical model was constructed. The model is based on the commercial CFD software Flow3D. As a first approximation the redistribution of particles by the interaction of density differences and general flow patterns induced by the pouring process was considered. At

this stage of the model development, some relevant physical phenomena such as thermal buoyancy, mechanical impact of burner flame and particle agglomeration and loss to the furnace walls were neglected. These factors will be progressively integrated into the model in future work. Currently, the model considers the melt as isothermal and describes only flow patterns induced by the tilting motion of the furnace and the draining of the vessel.

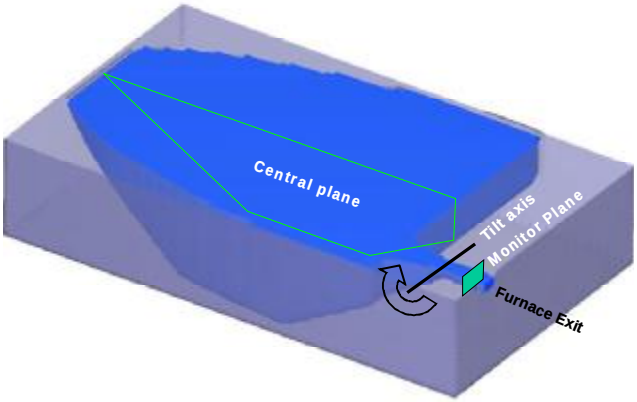

Figure 2. Furnace geometry used in current study

The model takes advantage of the so called "General Moving Obstacle" method [1], to describe the tilting of the furnace in space. In this description, geometric entities are rotated through a fixed numerical grid. Compared to methods with a rotating force vector this approach has two main advantages: It can be easily combined with a non-rotating launder while maintaining alignment the grid with the upper melt surface. To reduce calculation time, the free melt surface on top of the melt was approximated by a rigid wall with a slip condition. Numerically, this constrains the melt motion avoiding the occurrence of time step limitations due to surface waves. In the simulation the furnace rotation is controlled by a function for the angular velocity to achieve an essentially constant flow rate at the furnace exit.

The particles in the melt are described by discrete Lagrangian points, which are tracked throughout the calculation. The particles are not considered to interact with each other. Since the absolute particle concentration is very small, this restriction should have no serious consequences. Compared to scalar inclusion concentration the discrete approach has advantages in terms of reduced computational costs. Even on a coarse grid comparatively detailed information of the particle motion can be achieved. Enrichment of particles can be observed even in fractions of a computational cell. In principle, it is very easy to consider a size distribution of the particles, as an increase in the number of equations considered is not required. To model the particle motion in the 45t furnace under consideration about 150000 Lagrangian particles were used in the simulation. This produced a reasonable statistical distribution of particles at the furnace exit.

A limitation in the code is that either the particle sizes or the particle densities can be varied in one calculation but not both simultaneously. Therefore, several calculations were performed in order to evaluate the experimental matrix of Table 2. Usually 4 classes of different particle diameters or particle densities were considered in each simulation. Thus a range of virtual densities from particles with attached bubbles to dense aluminium oxide inclusions in the range 25 – 55µm was covered.

Table 2. Experimental matrix evaluated in this study

Physical properties of simulated particles				
Size	Density			
25µm	700 kg/m^3	1800 kg/m^3	2900 kg/m^3	4000 kg/m^3
35µm	700 kg/m^3	1800 kg/m^3	2900 kg/m^3	4000 kg/m^3
45µm	700 kg/m^3	1800 kg/m^3	2900 kg/m^3	4000 kg/m^3
55µm	700 kg/m^3	1800 kg/m^3	2900 kg/m^3	4000 kg/m^3

Most of the calculations for this study were performed on a grid consisting of either about 15 or 60 thousand active cells. An assessment of the sensitivity of the results to the size of the computational grid used was made by expanding the grid to ca. 150 thousand cells and comparing the results of identical simulations the three different sized grids as and shown in Figure 9. A calculation with a cell number of 15000 and 150000 particles took about 5.5 hours of CPU time on an Intel Xeon 5160 processor (3GHz).

The simulation results were analysed using the following two methods:

1. A monitoring plane across the furnace exit as shown in Figure 2 was used to count the particles within the four classes exiting the furnace. From this integral particle number the particle fluxes (counts per time) were computed and finally normalized with the volume flow rate to achieve the particle concentration at the furnace spout.
2. The spatial distribution and motion of particles were analysed using video animations of furnace tilting to visualise the main patterns of particle motion.

Industrial Reference

Typical LiMCA curves which may be expected depending on the length of time previously available for particle settling, the overall level of inclusions in the melt and the degree to which the furnace is emptied during casting are given in Figure 3 and Figure 4 as references for the comparison with the simulation results. Similar LiMCA results have been previously reported [2-3].

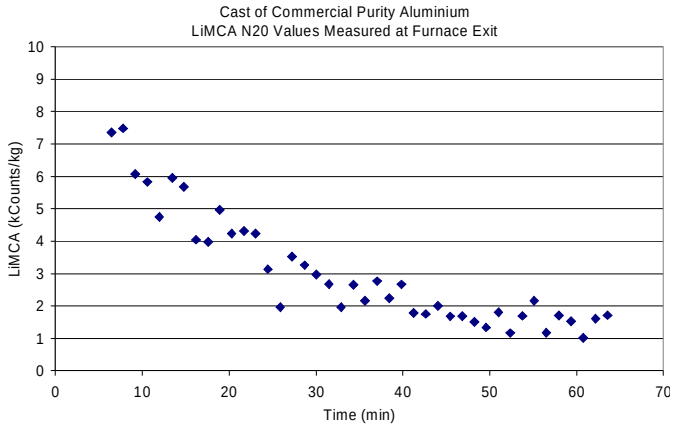

Figure 3. Typical LiMCA curve showing inclusion concentration in the metal at the furnace exit during casting. Note the decreasing numbers of inclusions due to settling behaviour of particles with time

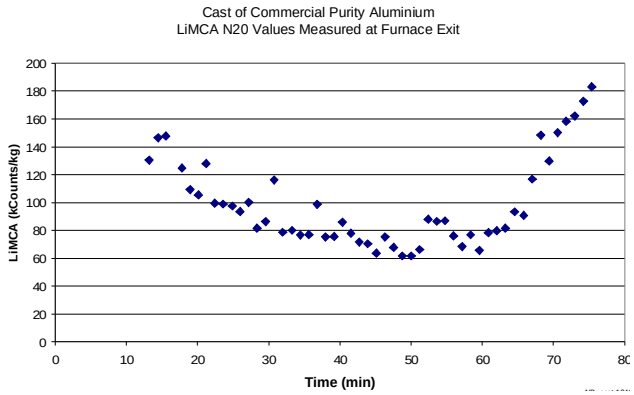

Figure 4. Typical LiMCA curve showing inclusion concentration in the metal at the furnace exit during casting. Note the increasing number of inclusions towards the end of the cast as the inclusion rich liquid is expelled from the furnace

Of interest in this initial development of the model was the degree to which the simulation could reproduce these types of curves, which are typically observed in industrial operations.

Results

The presentation and discussion of the results will be limited to the simulations shown in Table 3 and the effect of grid size on the simulation output.

Table 3. Parameter settings for the various simulations included in the current study

Case No.	Computing Parameter	Fixed Parameter	Variable Parameter				
1	60k cells 150k particles	Particle size (25µm)	700	1800	2900	4000	kg/m^3
2	60k cells 150k particles	Particle size (55µm)	700	1800	2900	4000	kg/m^3
3	15k cells 150k particles	Particle density (700 kg/m^3)	25	35	45	55	µm
4	15k cells 150k particles	Particle density (4000 kg/m^3)	25	35	45	55	µm
5	15k cells 150k particles	Particle size (55µm)	700	1800	2900	4000	kg/m^3
6	150k cells 150k particles	Particle size (55µm)	700	1800	2900	4000	kg/m^3

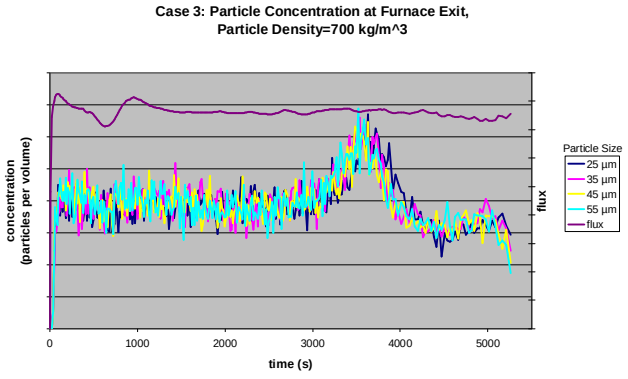

(a)

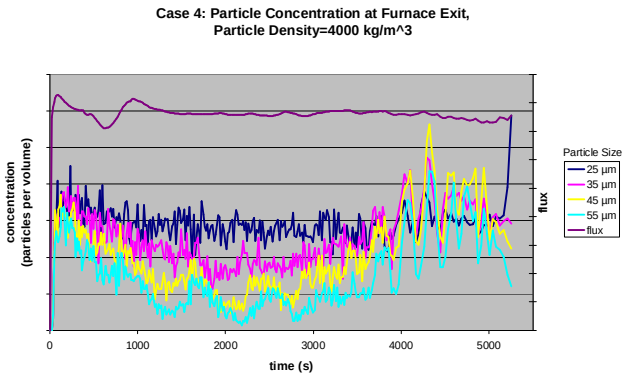

(b)

Figure 5. Effect of particle size for (a) 700 kg/m^3 (b) 4000 kg/m^3. At low densities, the particle size does not play an important role in determining particle movement patterns but becomes increasingly important at higher densities.

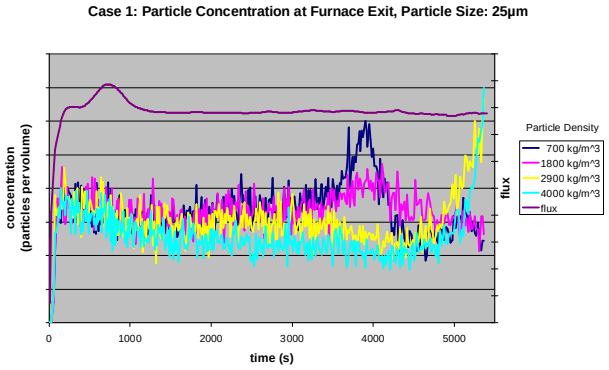

(a)

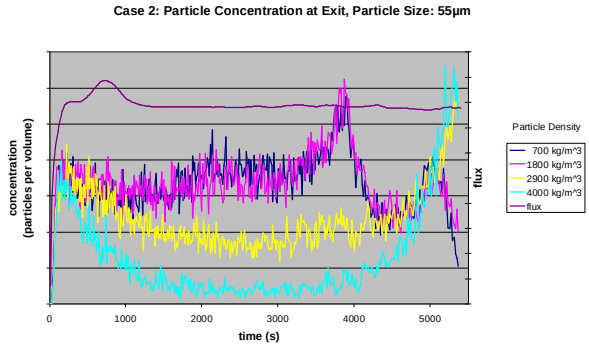

(b)

Figure 6. Effect of particle density on particle behaviour of 2 different sized particles (a) 25µm and (b) 55µm

Discussion

Figure 5 shows the different behaviour patterns of particles of different sizes. These results are presented for particles of two densities (a) 700 kg/m^3 and (b) 4000 kg/m^3. At low particle densities, the particle size (in the range considered) does not play an important role in determining particle movement patterns while at higher densities, the effect of particle size becomes increasingly important.

Figure 6 (a) und (b) show the variation in the concentration with time of particles passing the monitoring plane at the furnace exit for a constant flow rate (flux) of metal out of the furnace. A progressive segregation of particles due to density differences can be seen for both the 25µm and 55µm particles although this effect is more pronounced for the larger particles. A peak in particle flux for the less dense particles can then be seen in the time period 3000 to 4000 seconds in both Figure 6 (a) and (b). The emptying of the furnace and the particle movement patterns will be discussed with reference to the video capture images shown in Figure 7, which describe the results of Case 2 shown in Figure 6(b). Furnace geometry and distribution of particles within the stationary furnace at the commencement of the simulation is shown in Figure 7(a). Initially metal from the forward areas of the furnace flows out of the pouring spout with a relatively constant level of inclusions. Larger particles and more dense particles settle to the lower regions in the furnace and their numbers at the furnace spout decrease (Figure 7(b)).

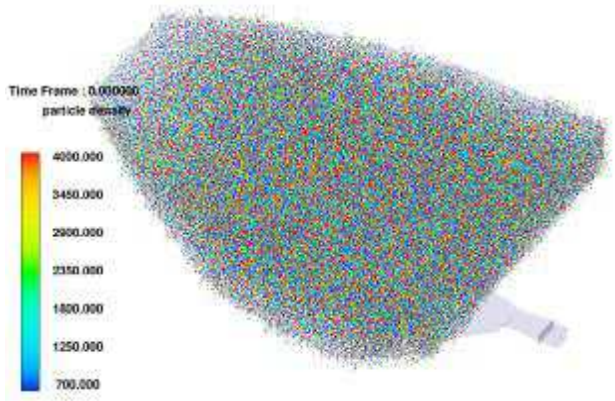

(a) Start of simulation 0 seconds

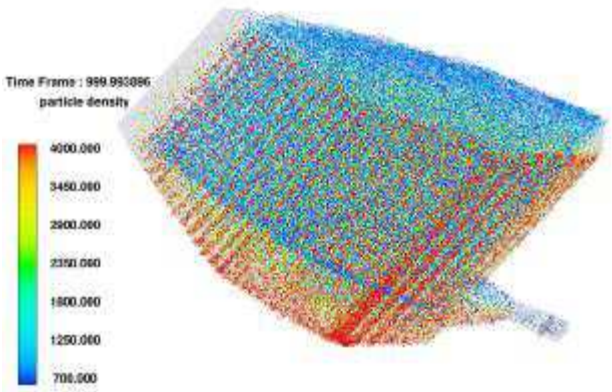

(b) 1000 seconds elapsed

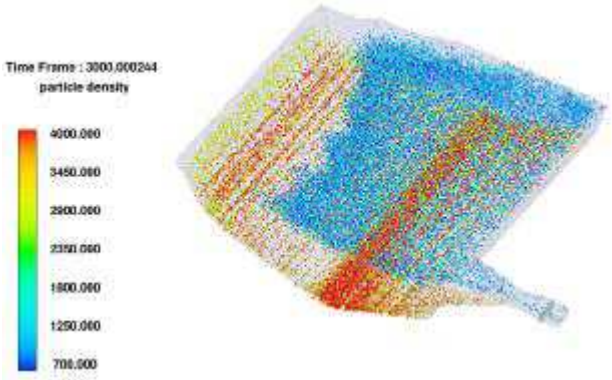

(c) 3000 seconds elapsed

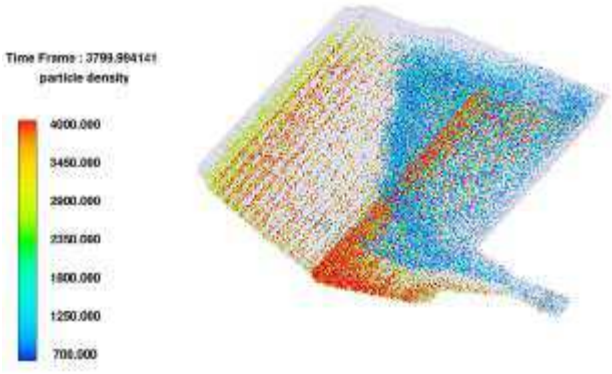

(d) 3800 seconds elapsed

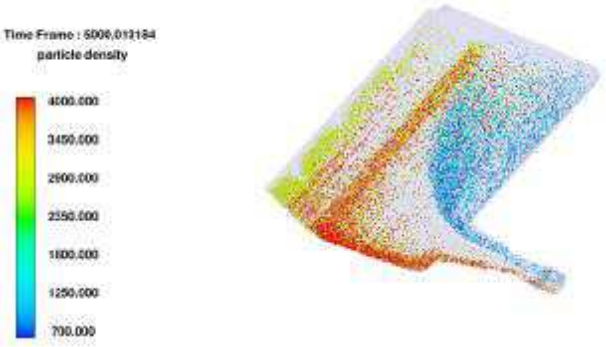

(e) 5000 seconds elapsed

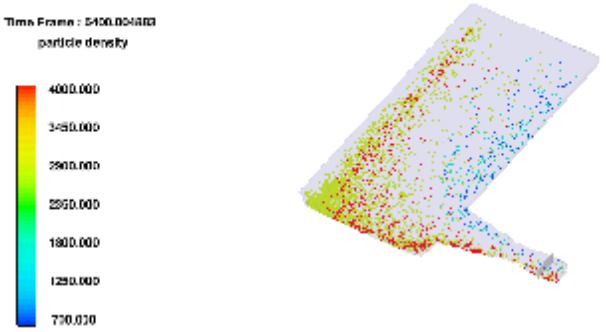

(f) End of casting simulation, 5400 seconds elapsed

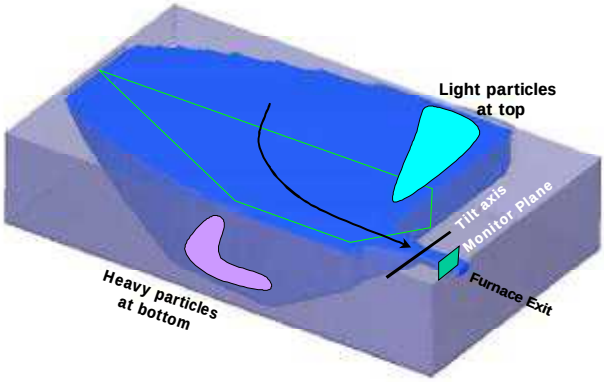

(g) Schematic diagram of particle accumulation zones resulting from the general fluid flow pattern.

Figure 7. 3-D Visualisation of casting simulation

The peak in particle flux for the less dense particles mentioned above can be explained in terms of particle settling behaviour and the contribution of the furnace geometry to the flow patterns within the melt during tilting of the furnace. The progressive exposure of the furnace bottom to the atmosphere due to the tilting of the furnace continuously brings metal from the bottom of the furnace to the surface of the melt at the rear of the furnace. This material is enriched in denser particles and contains relatively few particles of low density. It flows along the surface of the melt towards the furnace spout with a high local velocity accelerating the metal ahead of it, which is rich in inclusions of low density. Velocity vectors at 3000 seconds for this simulation are shown in Figure 8. The red zone at the melt surface shows the area of accelerated melt flow. The surface region in the middle of the furnace thus becomes enriched in low density particles (Figure 7(c) and Figure 8). At some point this material too flows out of the furnace and a peak in the numbers of low density particles is observed at the monitoring plane (at about 3800 seconds in this case Figure 7(d)). Only very few high density particles are detected at the furnace exit at his time as they have had sufficient time to sink to the bottom of the furnace again. The remaining metal in the furnace is either that which has been brought to the surface with progressive tilting of the furnace and that, which has remained on the floor in the deepest areas of the furnace. This metal is enriched in high density inclusions and depleted of low density inclusions. Towards the end of the cast the remaining metal is expelled from the furnace and a peak in high density particles at the furnace exit is detected Figure 7(e). It is thus possible to identify zones where less dense and denser particles would tend to accumulate (Figure 7(g)).

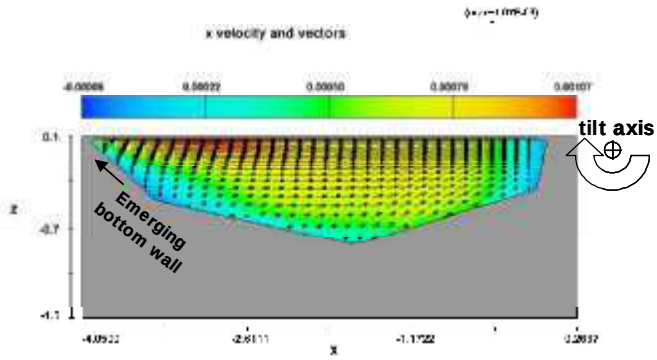

(a)

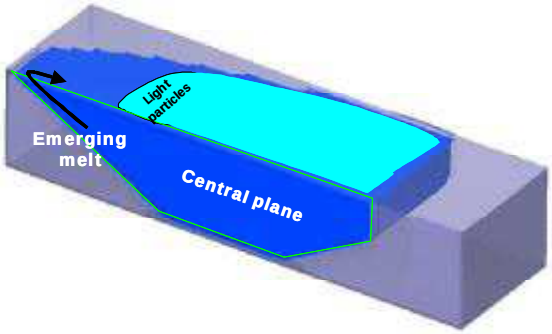

(b)

Figure 8. (a) Velocity vectors at 3000 seconds for Case 2 in the central plane of the furnace showing high flow rates on the surface of the melt. (b) Schematic diagram showing concentration effect of low density particles due to fluid flow on the surface of the melt. The driving force for this velocity maximum on the melt surface is the emerging bottom wall. These results are also shown also in Figure 6(a) and Figure 7.

Several checks were made for internal consistency of the model. Some parameter values were repeated in the various simulations. For example 25µm particles of density 700kg/m^3 are included in simulation one and three and 55µm particles of density 4000kg/m^3

are included in simulations two and four of Table 2. Therefore the curves for these particles should be the same in Figure 6(a) and Figure 5(a) and Figure 6(b) and Figure 5(b) respectively. As can be seen in the figures the agreement is quite reasonable. The results do show a dependency on the grid size. This can be easily seen in Figure 9. Here the simulation using identical parameters has been repeated for three different grid sizes of approximately 15k, 60k and 150k cells (cases 2, 5 and 6 respectively). For practical purposes the intermediate mesh size appears to be sufficient. It provides sufficient resolution and improved stability over the large mesh size while requiring significantly less processor time than the finest mesh (36 hours processing time compared to 60 hours).

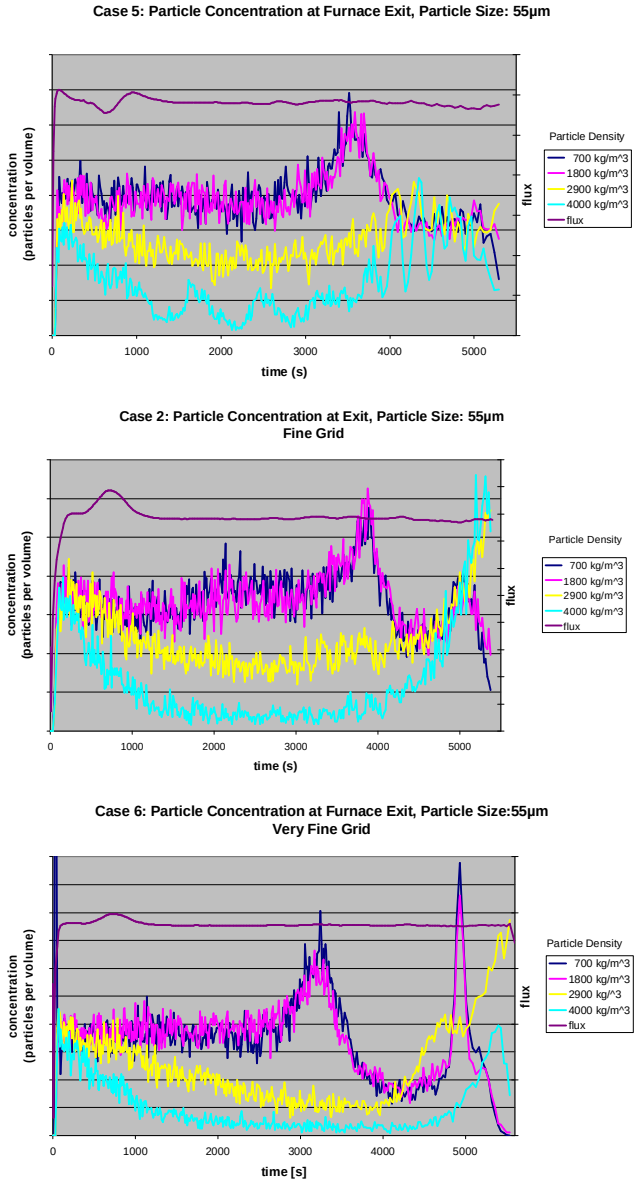

Figure 9. Effect of computational grid size on simulation output.

Conclusions

A model has been developed to simulate the fluid flow phenomena and behaviour of suspended particles in an aluminium melting or holding furnace. This model was used to evaluate fluid flow and particle segregations during tilting and emptying of a furnace. The important behavioural characteristics dictated by the relevant physical laws governing buoyancy and fluid flow, etc. are reproduced by the model. The numerical model showed characteristic particle segregations, which did not result from gravity effects alone, but were also the result of the flow patterns induced by the tilting and draining of the furnace.

- A progressive segregation of particles due to density and size differences was identified.
  - Particle classes with densities greater than that of the melt sank to the bottom of the furnace and particle classes with a lower density migrated to the surface of the melt.
  - For the lowest particle densities (700kg/m3 and 1800 kg/m3) particle size was not a significant factor influencing particle migration patterns.
  - Particle size appears to be more significant for particles with densities greater than that of the melt. As expected, the large particles (55µm) showed the strongest segregation patterns and deviations from the average concentration in the furnace spout.
- The furnace geometry could be shown to have a significant influence on the fluid flow and particle distribution patterns:
  - The flow pattern is mainly influenced by the shape and tilt axis position of the furnace. This determines where particles will accumulate in the furnace and when these enriched or depleted volumes will exit the furnace.
  - Peaks and troughs in the numbers of the various classes of particles were detected at the furnace exit at various times in the simulation as a result of settling and furnace geometry effects. This resulted in lighter particles being washed out of the furnace more quickly than the heavier particles.

It is planned to progressively refine the model to include such important aspects as:

- Gas burner impact
- Thermal convection
- Sedimentation
- Particle interaction with furnace walls

References

[1] Flow3D 9.2, *User Manual* (Flow Science Inc, Santa Fe (NM)).

[2] J. P. Martin, R. Hachey and F. Painchaud, *On-Line Metal Cleanliness Determination in Molten Aluminium Alloys* (Light Metals 1994), 915-920.

[3] Nick Towsey, Wolfgang Schneider and Hans-Peter Krug, *The Effect of Rod Grain Refiners with Differing Ti/B Ratios on Ceramic Foam Filtration (* Light Metals 2002), 931-936.